V. PHYSICAL ACOUSTICS[*]

Academic and Research Staff

Prof. K. U. Ingard
Dr. C. Krischer

Graduate Students

A. G. Galaitsis
G. F. Mazenko

P. A. Montgomery
J. A. Ross, Jr.

A. ULTRASONIC DISPERSION IN PIEZOELECTRIC SEMICONDUCTORS

The interaction between an ultrasonic wave and the mobile charge carriers in a piezoelectric semiconductor can result in dispersion, as well as amplification, of an elastic wave. A linear, small-signal, macroscopic theory that is valid in the regime in which the acoustic wavelength is much larger than the electron mean-free path has been presented by Hutson and White.[1,2] White[2] has given an expression for the dependence of the ultrasonic velocity on the electrical conductivity and the electron drift velocity:

$$v_s = v_o \left\{ 1 + \frac{K^2}{2} \left[\frac{\gamma^2 + \frac{\omega_c}{\omega_D}\left(1 + \frac{\omega^2}{\omega_c \omega_D}\right)}{\gamma^2 + \left(\frac{\omega_c}{\omega}\right)^2 \left(1 + \frac{\omega^2}{\omega_c \omega_D}\right)^2} \right] \right\},$$

where

$v_o = (c^E/\rho)^{1/2}$ = "unstiffened" phase velocity

K = electromechanical coupling constant

$\omega_c = \sigma/\epsilon$ = conductivity relaxation frequency

σ = electrical conductivity

$\omega_D = (e/kT)v_o^2/f\mu$ = diffusion frequency

μ = electron drift mobility

f = trapping factor = fraction of space charge which is mobile

$\gamma = 1 - v_d/v_o = 1 + f\mu E_d/v_o$ = drift parameter

E_d = applied electric drift field

ω = elastic wave angular frequency.

The range of possible phase velocities lies between $v_D = v_0(1+K^2)^{1/2} \approx v_0(1+K^2/2)$ and v_0. In the limit of small conductivities and large values of drift parameter, the charge carriers cannot effectively "cancel out" the longitudinal electrostatic field of piezoelectric origin that is produced by the ultrasonic wave, and therefore v_s approaches the fully stiffened velocity, v_D. Conversely, in the limit of high conductivity and small drift parameter, there does occur effective electron bunching which cancels out the piezoelectric field; hence, v_s approaches the unstiffened velocity v_0. For any given conductivity, v_s has a minimum value when $\gamma = 0$, that is, when the electron drift velocity equals the sonic velocity.

We are now investigating the dependence of the phase velocity in CdS on the electrical conductivity and applied drift field. Our sample dimension is 1 cm along the direction of propagation and approximately 0.5 X 0.5 cm in cross section. The transverse-wave acoustic pulses, propagating in the basal plane with polarization along the c axis, are generated and detected by two 32-MHz Y-cut quartz transducers bounded to the sample ends. The complete delay line is mounted in a holder in thermal contact with a thermoelectric module, and its temperature is maintained at 20 ± 0.2°C.

The total insertion loss for the delay line (with the ultrasonic attenuation minimized by keeping the CdS sample in the dark) varies from 20 dB at the fundamental frequency (32 MHz) to 50 dB at the 13th harmonic (410 MHz). We shall therefore be able to obtain data over a wide range of frequencies. The electrical conductivity is adjusted by varying the light intensity from a tungsten-filament quartz-iodine lamp powered by a regulated DC supply. A range of more than four orders of magnitude variation in the conductivity is obtained. A pulsed, low duty-cycle drift field is used to minimize the errors caused by heating. (For example, at 20°C, a temperature change of ±1°C results in an observed apparent velocity change of ±0.01%). The variations in phase velocity are measured by using a standard phase-interference technique. The input radiofrequency is adjusted so that the delayed output signal interferes destructively with the input signal. The relative velocity changes are thus measured as relative changes in the null frequency.

Figure V-1 shows the results of measurements carried out at 94 MHz. Data could not be obtained for the medium conductivities at drift fields below 500 V/cm because the ultrasonic attenuation in this region is too large: the signal is masked by the presence of a piezoelectrically inactive acoustic wave (polarized in the basal plane), whose phase velocity is very nearly equal to that of the active wave. The data for large conductivities at the higher drift fields were limited by the build-up of ultrasonic flux. The total range of velocity variation corresponds to a value of $K^2 = 0.035$, which compares very favorably with the value of 0.036 reported by Hutson and White.[1] Our results differ significantly
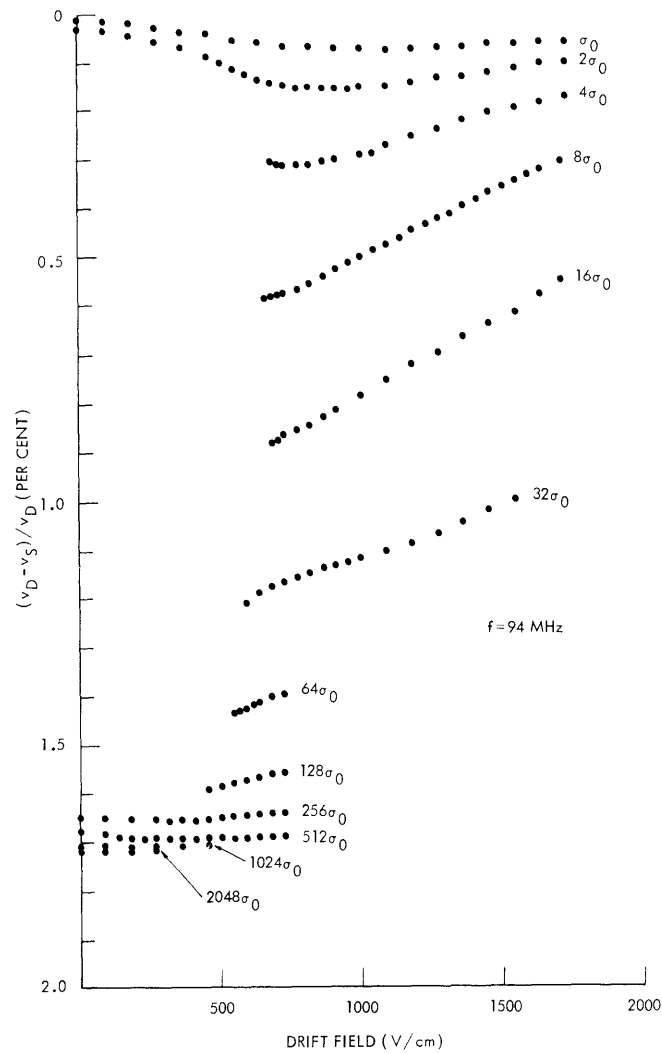
Fig. V-1. Variation of phase velocity with electrical conductivity and applied drift field for a 94-MHz piezoelectrically active transverse wave in CdS ($\sigma_O \approx 10^{-5}$ $(\Omega\text{-cm})^{-1}$).

from the predictions of Hutson and White's theory in one respect: the drift field corresponding to minimum velocity decreases monotonically with increasing conductivity. We shall attempt to determine whether these results are consistent with the assumption of a complex trapping factor which occurs when the equilibration time of the trapped electrons is of the same order of magnitude as the elastic wave period. (Ishiguro and co-workers[3] have shown that the observed asymmetry in the ultrasonic gain-loss vs drift field curves results from a complex trapping factor.)

C. Krischer

References

1. A. R. Hutson and D. L. White, J. Appl. Phys. 33, 40 (1962).

2. D. L. White, J. Appl. Phys. 33, 2547 (1962).

3. T. Ishiguro, I. Uchida, T. Suzuki, and Y. Sasaki, IEEE Trans., Vol. SU-12, p. 9, 1965.

B. NONLINEAR INTERACTION BETWEEN A SOUND FIELD
   AND A LIQUID SURFACE

1. Static Pressure Distribution in Sound Field

It follows from the Navier-Stokes equation that the time average of the pressure in a one-dimensional sound field is given by $\langle p \rangle = -\langle \rho u^2 \rangle + \text{const}$, where ρ is the density, and u is the velocity. Thus, if u_1 represents the first-order velocity field obtained from the linearized equations of motion, the time average of the pressure, correct to second order, is $\langle p_2 \rangle = -\rho_0 \langle u_1^2 \rangle + \text{const}$, where ρ_0 is the unperturbed density.

Applying this result to a standing wave in a closed tube, we find that the spatial distribution of the time average or static pressure in the sound field is of the form $\langle p_2 \rangle = \left(p_{10}^2 / 4\rho_0 c^2 \right) \cos(2kx) = p_{20} \cos 2kx$, where $(2\pi/k)$ is the wavelength, p_{10} the maximum first-order sound pressure amplitude in the standing wave, and c the speed of sound.

This pressure distribution can be demonstrated in a simple manner by letting this sound-pressure field act on a horizontal liquid surface parallel with the x direction. This interaction results in a vertical displacement of the surface which varies with x as $\cos(2kx)$, as shown in Fig. V-2. At sufficiently high levels of the sound pressure the
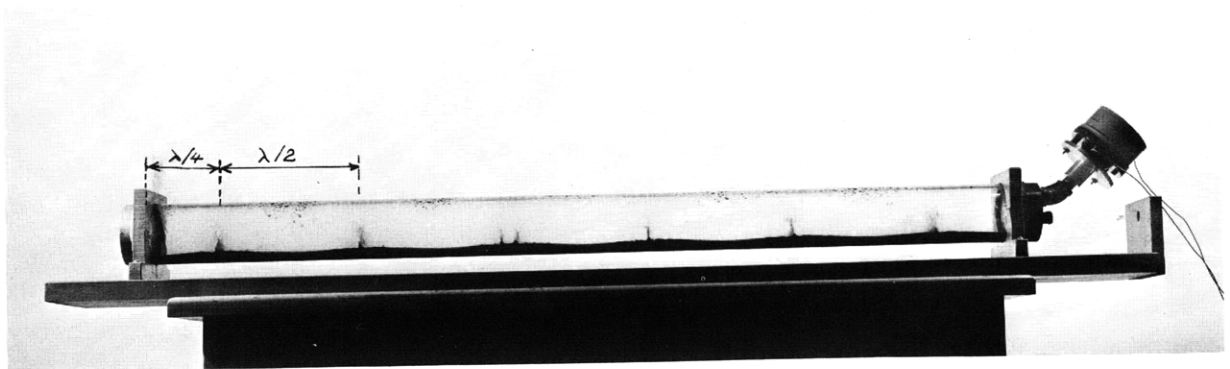

Fig. V-2. Demonstration of the time average (static) pressure distribution in a standing sound wave and the acoustic fountain effect.

surface is ruptured and "fountains" occur at the pressure nodes. This also can be seen in Fig. V-2.

This phenomenon has been known for a long time,[1] but no satisfactory explanation of the fountain effect has been given. Questions that relate to the conditions for the onset of the fountain such as threshold sound pressure have not been answered.

In order to try to better understand this phenomenon, we have studied sound-liquid surface interaction, using cavities of different shapes and with liquids of several different viscosities and surface tensions.

The most extensive measurements were made in cylindrical cavities 38 in. and 15 in. long with inner diameters of 1 3/4 in. and 1 3/8 in., respectively. The cavities were driven at one end by a loudspeaker, and at the other end a microphone was mounted flush with the rigid end wall. The driving frequency was kept below the cutoff frequencies of higher duct modes so that only the plane-wave component was generated. The static pressure distribution in the sound field was measured by means of a sloping tube manometer, and the surface deformation was determined by a cathetometer. A sound-pressure level of 164 dB could be produced at various tube resonance frequencies
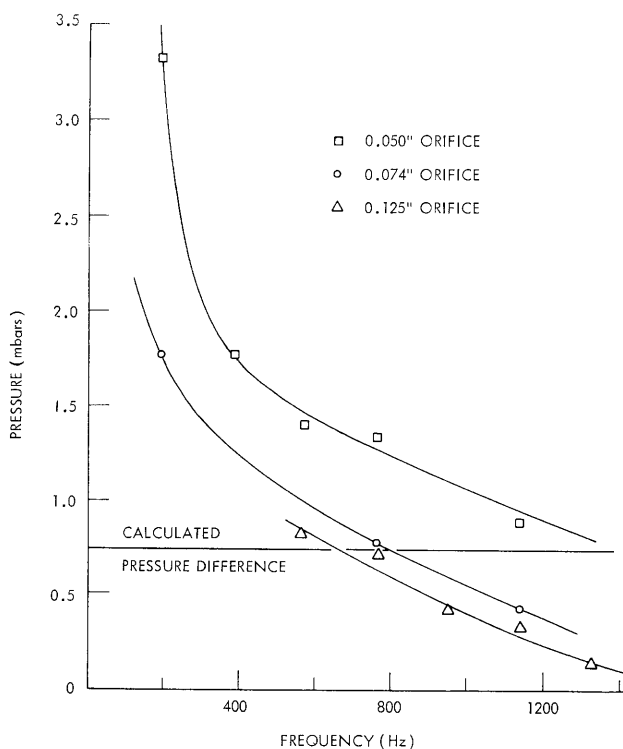

Fig. V-3. Pressure difference between antinode and node as measured with the manometer at a sound level of 164 dB. Results for three different probe orifice diameters are shown.

between 200 Hz and 1200 Hz.

Measurements of the static pressure distribution by means of the manometer turned out not to be particularly accurate. It was found that the results were influenced by the size of the probe orifice of the manometer and also by the frequency. This is probably due to local distortion or diffraction of the sound field about the orifice. Accordingly, the time average pressure at the probe can be considerably different from the pressure in the plane-wave field. The frequency dependence of the manometer output for three different probe orifice diameters is shown in Fig. V-3. This second-order time average in the diffracted sound field will be explored in more detail in a separate report.

With the static second-order pressure distribution given by p_{20} cos (2kx), the height of the liquid surface should vary as

$$y = y_o - \{p_{20}/\rho_L g(1+\zeta)\} \cos (2kx),$$

where

$$\zeta = \frac{(2k)^2}{\rho_L g} \sigma \quad \text{and} \quad p_{20} = \frac{p_{10}^2}{4\rho c^2},$$

with ρ_L = density of liquid; g = acceleration of gravity; σ = surface tension; and p_{10} = sound pressure amplitude. The difference in height of the liquid surface at the antinode and at the node is then $2p_{20}/\rho_L g(1+\zeta)$. Measurement of this difference was made in the 38-in. cavity (water depth ~1.5 cm) at a maximum sound-pressure level of 163.3 dB and at frequencies between 200 Hz and 1200 Hz. For water at 20°C the measured height difference was found to be independent of frequency and equal to 0.55 cm, with a standard deviation of 0.03 cm. This is in excellent agreement with the calculated value 0.54 cm.

2. Fountain Effect

If the sound level exceeds a certain threshold value, the liquid erupts suddenly at the antinodes, and this eruption, or fountain effect, is maintained by the sound field. Below the threshold the liquid surface is deformed as described above. There is no other distortion of the surface, however, which would indicate that the surface might erupt. The threshold sound level does not depend on the cross-sectional tube area of the region above the liquid surface, nor upon the frequency in the region considered, between 200 Hz and 2000 Hz. The threshold level depends, however, on the surface tension and the density of the liquid.

When the fountains are formed, the liquid surface is distorted by the static pressure distribution before the eruption. The question arises about the role of this initial distortion in the formation of the fountain. To check this, the liquid surface was replaced

with a flat solid block with the exception of a small region, a groove, near a pressure antinode. The liquid in the groove would suddenly begin to spray out of the groove when the threshold sound level was reached. This continued until the groove was very nearly empty. Thus we conclude that the over-all shape of the liquid surface as affected by the static pressure distribution is not an important factor in the formation of fountains.

It is difficult to determine the threshold of the sound pressure above which fountains occur. One reason is that often no fountains are formed immediately, even if the level exceeds the threshold determined from a previous experiment. A short time later (~1-10 sec), however, a fountain will erupt. Furthermore, the phenomenon exhibits "hysteresis"; the fountains, once started, can be maintained at a level below the threshold.
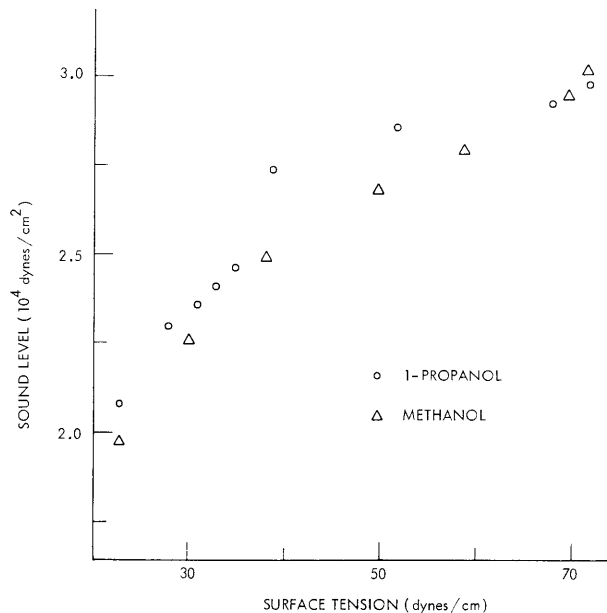

Fig. V-4.   Threshold sound level for fountain formation is shown as a function of surface tension.

Actually, if an initial distortion of the liquid is produced by touching it with a thin rod and then pulling the surface up to form a ridge, a fountain can be produced and maintained after removal of the rod, at a level approximately 20% below the actual threshold. The threshold determined in this manner was quite reproducible and could be accurately determined. In Fig. V-4 this threshold is shown as a function of the surface tension of two-component systems of propanol-water and methanol-water. The surface tension was varied by varying the concentration of these liquids. This clearly shows that the threshold increases with surface tension.

a. Mechanism of the Fountain Effect

As has already been demonstrated, the explanation of the fountain effect does not appear to lie in the static deformation of the liquid surface and the corresponding axial pressure gradient of the plane-wave sound field. A possible cause of the fountain effect, suggested by Sanders,[2] is the coupling between the acoustically produced vortex flow (acoustic streaming) and the liquid through the viscous stress at the surface. But restricting the liquid only to a very small region, as we did in our experiments with the liquid in a small groove, would no doubt reduce this coupling; yet the threshold for the fountain effect was found to be unchanged as we have mentioned. Therefore, this "viscous drag" mechanism is not consistent with the experimental results.

Another possible explanation is related to the periodic change in the tube cross section caused by the periodic deformation of the liquid surface. Such a change in cross section would increase the velocity in the constricted regions, decrease the static pressure, and thus raise the liquid surface further in these regions. This mechanism is not consistent with the observation that the fountain occurs at the same threshold level practically independent of the water level, and also that a fountain occurs too when the liquid is placed in a small groove in an otherwise flat surface. An extension of this idea, having to do with the acoustic scattering from a small irregularity in the liquid surface, appears to be the most likely mechanism. A scattered wave at a small ridge in the liquid surface will increase the acoustic particle velocity at the top of the ridge, and hence decrease the static pressure there. This will amplify the ridge and, in turn, this will increase the scattered field. This process would continue until the decrease in pressure is sufficient to overcome the restoring force of surface tension and gravity to rupture the liquid.

To explore the feasibility of this mechanism, we consider the scattered field about a rigid cylinder in an incident plane wave. From this well-known result[3] we readily obtain the scattered field and the total velocity distribution about a semicylindrical ridge in a plane boundary. If the cylinder radius r_o is small compared with the wavelength, $kr_o \ll 1$, the result is particularly simple, and the corresponding static pressure decrease at the top of the cylindrical ridge is found to be four times as large as in the absence of the ridge. As a result of this static pressure distribution, the cylindrical ridge will be sharpened at the top so that its radius of curvature will decrease and the cylindrical boss will be deformed into a shape approaching a thin vertical wall. This will lead to a further increase in the particle velocity at the ridge until the liquid erupts. In order to demonstrate the enchancement of the static pressure change in the sound field as a result of the diffracted field, rigid objects simulating ridges were inserted in the tube and exposed to sound. The static pressure distribution about these objects was measured by means of the manometers. (Since we were interested here only in relative values of the pressure, the problem regarding the absolute calibration was not important.) The results
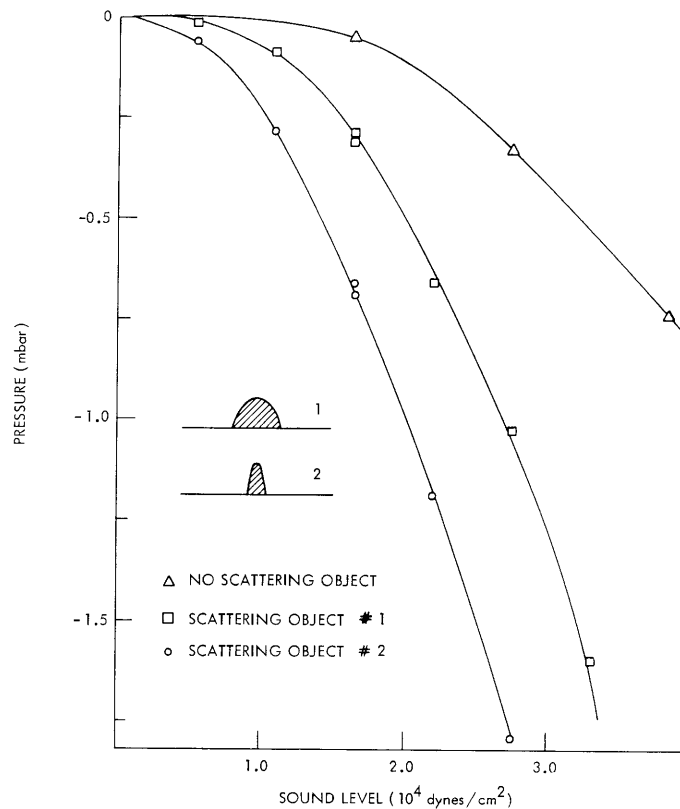
Fig. V-5. Pressure above scattering objects at an antinode shown as a
function of sound level.

are shown in Fig. V-5, where the static pressure drop above the scattering objects is
shown as a function of the sound pressure. The successive stages in the development
of a fountain are shown in Fig. V-6. We used a very viscous fluid (glucose in the form
of "Karo" syrup) so that the fountains would develop slowly. In fact, it was possible to
maintain at equilibrium the intermediate stages of the ridges shown in Fig. V-6.

Our experiments indicate that the dimension of a liquid ridge which is supported by
the sound field has typically a height of $h = 0.5$ cm and radius of curvature $r_o = 0.1$ cm.
The force per unit area required to maintain this ridge is $(\sigma/r_o) + \rho_L gh \approx 730 + 490 \approx$
1200 dynes/cm^2. To get an idea of the sound pressure required to maintain this ridge,
we use the result for the static pressure at the top of a cylindrical ridge. Since this
pressure is four times the unperturbed value, we get for the determination of the
(threshold) sound pressure p_{10} the relation (4-1)$\langle p_2 \rangle = 3p_{10}^2/4\rho_o c^2 = 1200$. This gives
$p_{10} \approx 4 \cdot 10^4$ dynes/cm^2, which corresponds to a sound-pressure level of approximately
163 dB. This is within a decibel of the observed threshold, and the scattering mech-
anism at least on this point is consistent with observations.

The question of how the ridges or surface perturbations are initiated still remains.
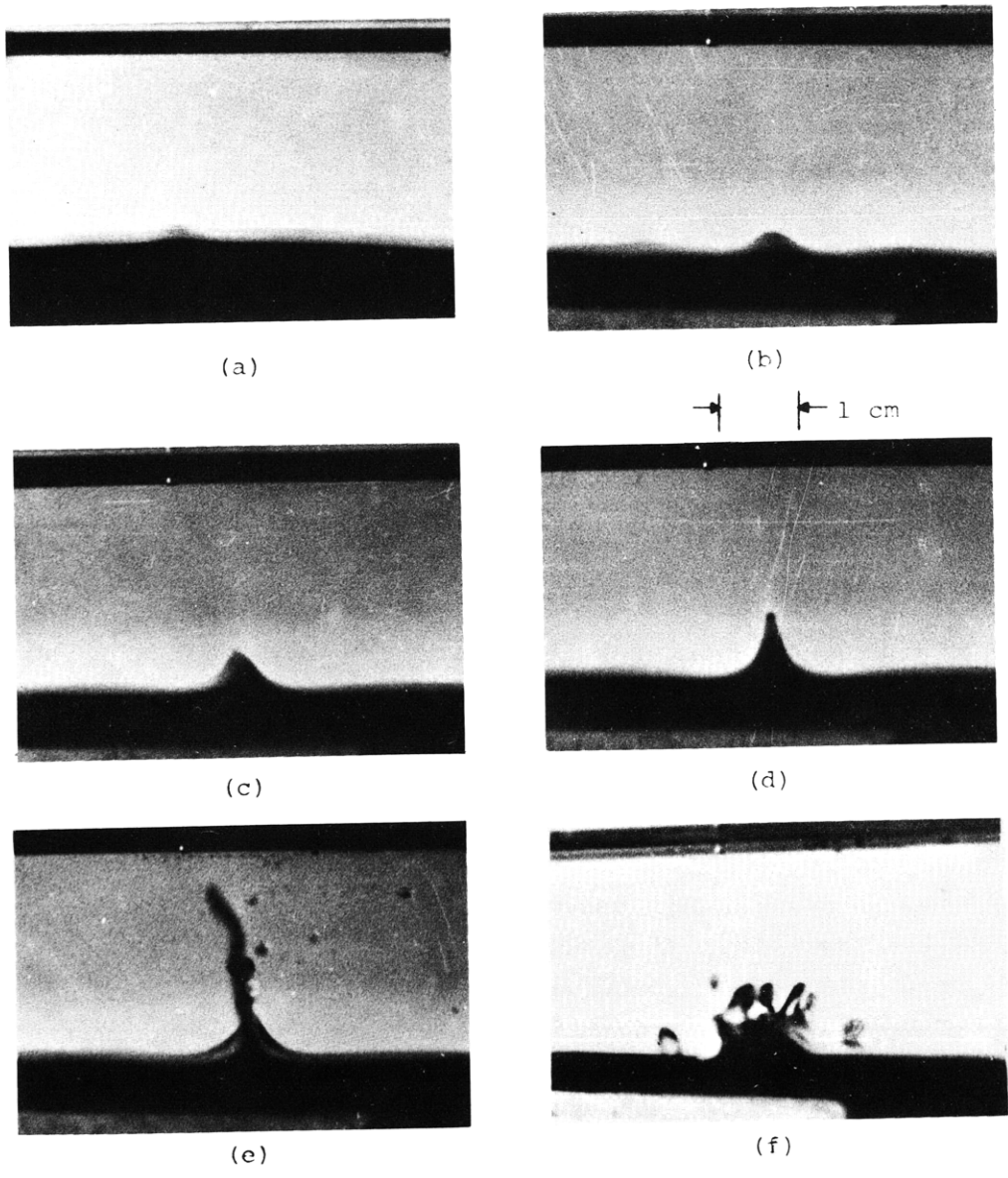
(a)

(b)

⊢⊣ ⊢ 1 cm

(c)

(d)

(e)

(f)

Fig. V-6. Successive stages of fountain formation are shown in (a), (b), (c), (d), and (e). The formation of droplets on top of the fountain ridge is shown in (f). These droplets will break loose and travel upward, thereby forming the actual fountain.

The scattering mechanism can only amplify an existing perturbation but cannot initiate it. Is a finite initial perturbation required for the instability to occur? One can get a rough idea about this problem by considering an initial semicylindrical perturbation of radius r_o. The pressure differential required to maintain such a perturbation must balance the restoring forces caused by surface tension and gravity. The first, σ/r_o, is inversely proportional, and the second is proportional to r_o. Thus, for sufficiently small perturbations the effect of surface tension dominates. Then, unless the perturbation is so large that the pressure differential $3p_{10}^2/4\rho_L c^2$ exceeds the equivalent pressure of surface tension, σ/r_o, an initial perturbation cannot grow. In other words, the required initial perturbation depends on the sound pressure in the tube. For a sound-pressure level of 163 dB the required perturbation is approximately 0.05 cm. Thermal fluctuations cannot and room vibrations are not likely to produce fluctuations of this magnitude. A probable source of the fluctuations is turbulence in the acoustically generated streaming (vortex flow) in the tube.

U. Ingard, J. A. Ross, Jr.

References

1. V. Dvorak, Ann. Physik 3, 102 (1874); V. Dvorak, Ann. Physik 7, 42 (1876); Lord Rayleigh, Phil. Trans. Roy. Soc. (London) A175, 1 (1883); E. N. da C. Andrade, Proc. Roy. Soc. (London) A134, 443 (1932); E. N. da C. Andrade, Phil. Trans. Roy. Soc. (London) A230, 413 (1932).

2. J. V. Sanders, Ph. D. Thesis, Cornell University, 1961, p. 98 (Univ. Microfilm 61-6764).

3. P. M. Morse and K. U. Ingard, Theoretical Acoustics (McGraw-Hill Book Company, New York, 1968), Chap. 8, p. 401.

C. NONLINEAR WAVE DISTORTION OF ACOUSTIC-NOISE SPECTRUM

As one part of our program in nonlinear acoustics we are considering the problem of the propagation of high-intensity acoustic noise, with particular emphasis on the nonlinear distortion of the power spectrum in a one-dimensional wave. The analysis is based on the hydrodynamic equations with the effects of viscosity and heat conduction omitted. An excellent survey of the application of these equations to sound propagation has been made by Blackstock,[1] who also gives an extensive list of references to previous work.

The particular problem with which we are concerned can be stated as follows: Assume that at a given position x = 0 the time dependence of the sound pressure can be expressed as a Fourier integral with the Fourier amplitude $P(\omega, 0)$ and a similar expression $V(\omega, 0)$ for the Fourier amplitude of the particle velocity. Assume that these quantities

are known, and determine $P(\omega, x)$ and $V(\omega, x)$ at some other position x. In a linear analysis, with viscosity and heat conduction omitted, these quantities are independent of x. Nonlinearity, however, introduces interaction between the various frequency components in the wave which leads to the generation of combination tones.

We shall not go through the details of the analysis here, but merely give the result obtained. We find that $V(\omega, x)$ can be expressed in terms of the integral

$$V(\omega, x) = \frac{2}{\pi} \int_0^\infty d\tau \int_0^\infty d\omega' \; V(\omega', 0) \; \sin \omega'\tau \; \sin \omega(\tau + F(x, \tau)) \frac{\partial t}{\partial \tau}, \tag{1}$$

where

$$F(x, \tau) = \frac{x}{c_0(1 + \alpha V_0(\tau))} \qquad (x \gg X_0)$$

$$t = \tau + F(x, \tau).$$

Here, $v_0(t) =$ particle velocity at $x = 0$; $X_0 =$ transducer displacement; $\alpha = \frac{\gamma + 1}{2c_0}$; $c_0 =$ unperturbed speed of sound; and $\gamma = \frac{c_p}{c_v}$.

The corresponding expression for $P(\omega, x)$ is obtained by replacing V with P in Eq. 1. In many cases the integration over ω' can be carried out analytically, but the τ integration must be done numerically. It should be pointed out that the solution given here refers to the case in which the velocity at $x = 0$ starts from zero at $t = 0$. In describing the behavior of a random field, we must consider an ensemble average over randomly chosen initial conditions. This question will not be considered in this report.

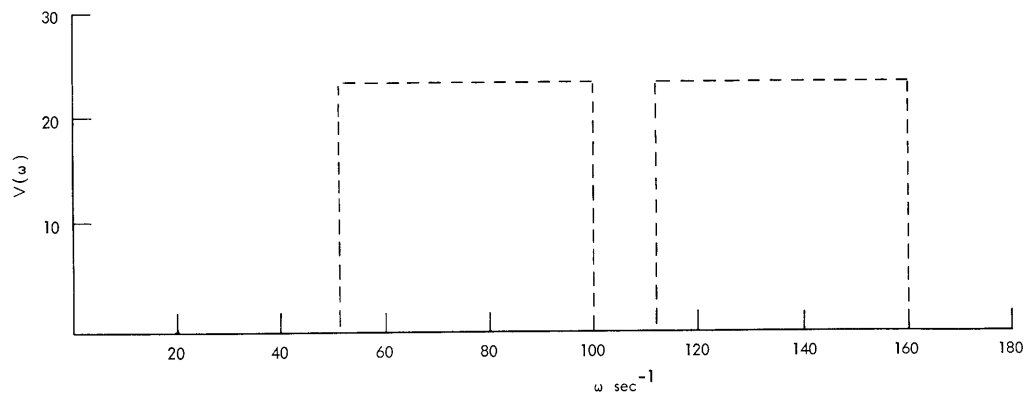Example. We apply the result obtained to a special case in which $V(\omega', 0)$ is

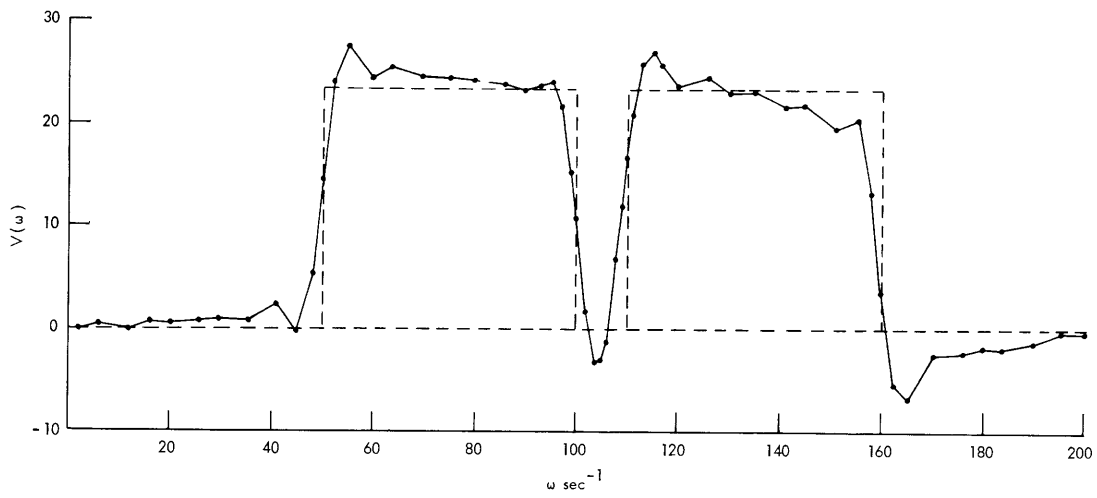Fig. V-7. Fourier spectrum at x = 0. Arbitrary scale for V(ω).

38

Fig. V-8. Fourier spectrum at x = 1. Arbitrary scale for V(ω).

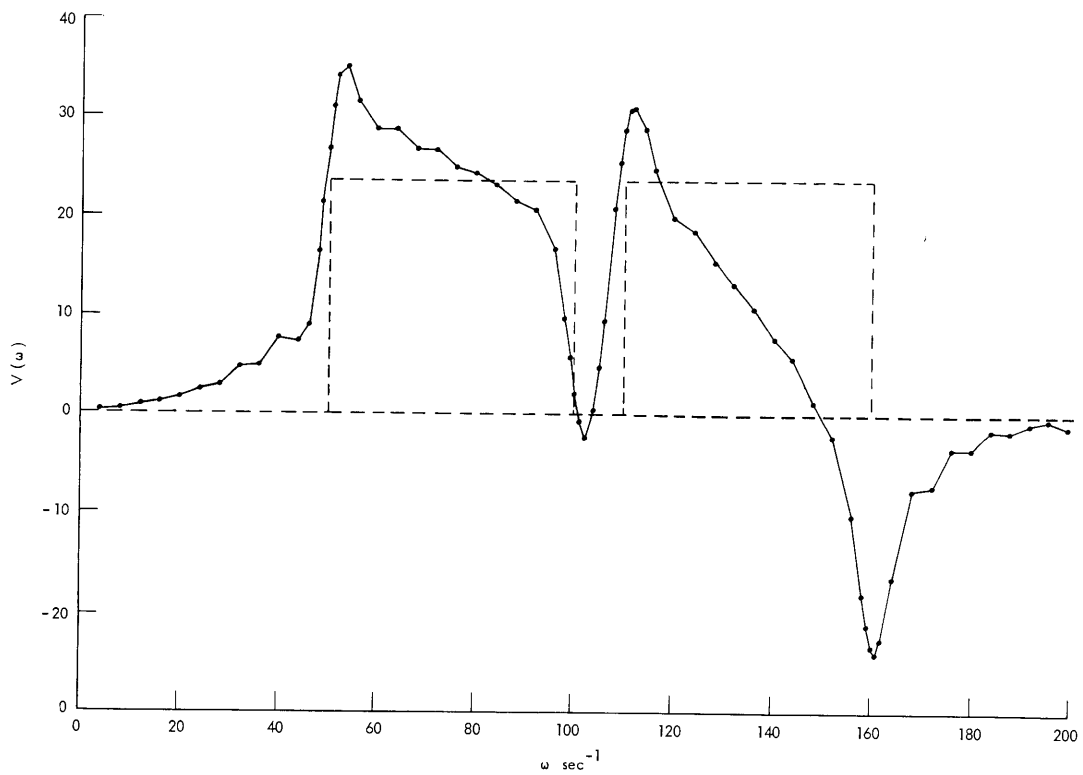Fig. V-9. Fourier spectrum at x = 2. Arbitrary scale for V(ω).

constant and real over a certain region of ω' except for a gap in the center of this region, where $V = 0$, as shown in Fig. V-7. We have chosen $V(\omega', 0) \, \Delta\omega = 0.01 \, c_o$, with $\Delta\omega = 1 \, sec^{-1}$, but this value has been normalized to unity in Figs. V-7, V-8, and V-9. These figures show the spectrum shape obtained from Eq. 1 at $x = 0$, $x = 1.0$, and $x = 5.0$ m.

<div align="right">G. F. Mazenko</div>

References

1. D. T. Blackstock, "Propagation and Reflection of Plane Sound Waves of Finite Amplitude in Gases," ONR Technical Memorandum 43, Acoustics Research Laboratory, Harvard University, June 1960.